On the Evolution of Shallow-Water Waves

Graceanne Paz, McNair Scholar
The Pennsylvania State University

McNair Faculty Research Adviser:
Diane M. Henderson, Ph.D.
Professor of Mathematics
Department of Mathematics
Eberly College of Science
The Pennsylvania State University

Abstract

This project studies the evolution of shallow-water waves for an initial-value problem using experiments, modeling, and analysis. To model the behavior of a wavetrain at a water surface, we compute solutions to the linearized boundary value problem for water waves. We solve for the dispersion relation between frequency and wavenumber and consider various limits of the solution. For shallow-water waves, we determine a soliton solution of the full KdV equation and solve the linearized equation with given initial conditions, relevant to the experiments. In the WGP Fluid Mechanics Lab, a system fabricated with a submerged plate abruptly moves horizontally to generate a soliton or vertically to generate an evolving wavetrain. We obtain measurements of the surface displacement as a function of distance from the plate using two capacitance-type wave gages. We compare the experimental results to predictions from our mathematical models. Analytic solutions of the KdV equation agree reasonably well with the measurements of the surface displacement obtained from the experiments on solitons. Analytic solutions of the linearized KdV equation provide qualitative insight into the observed evolution of the evolving wavetrains.

§I. Introduction

In this paper, we investigate analytically and numerically the evolution of waves at a water surface. The study focuses primarily on shallow-water waves, which describe waves for which the wavelength is long compared to the water depth. However, we first consider, in general, the dispersive effects and wave speed for waves in all depths of water. We conduct experiments, in which we generated waves by the pushing, dropping, and lifting of a plastic box, and obtained measurements of surface displacement. We compare these measurements with graphical representations of our solutions to the full and linearized KdV equation.

Stokes (1847) first postulated the boundary value problem (BVP) for water waves. Dean & Dalrymple (1991) provide the background in fluid mechanics required to derive these equations. Stewart (2007) imparts the mathematical tools required to derive the kinematic boundary conditions at the free surface. To make the BVP tractable, we follow Dean & Dalrymple (1991) who show how to linearize the BVP subject to weak nonlinearity. Consequently, their procedure corresponds to small-amplitude waves. We solve the governing equation with linearized boundary conditions using the method of separation of variables learned from Strauss (2008).

Additionally, Dean & Dalrymple (1991) discuss various limits of the resulting dispersion relation, including the deep-water limit, in which the waves are short compared to the depth, and the shallow-water limit. They show that using asymptotic analysis, one can approximate the BVP for waves in shallow water with an evolution equation for the free surface, called the Korteweg de Vries (KdV) equation. Using initial conditions relevant to the experiments analyzed herein, we solve the linearized version of the KdV equation, following Walsh (2011) and Hammack & Segur (1978), who previously conducted similar experiments in shallow water. We compare initial value solutions to the KdV equation with the wave experiments.

This paper is organized as follows. In §II, we describe the methods that we use throughout our research project. We present the boundary value problem for water waves in §III. First, we introduce the fully nonlinear problem and discuss its difficulties. Then, we show how to linearize the problem and find the linear solution, including the dispersion relation. In §IV, we focus on shallow-water waves. We find the soliton solution of the KdV equation and solve the linearized KdV equation with given initial conditions. We compare the experimental results to the corresponding solutions of the full KdV and linearized KdV equation.

§II. Methodology

For this project, we rely primarily on calculation, modeling, and analysis to develop insight into the evolution of surface water waves. We compute and interpret solutions to the linearized BVP for water waves and the KdV equation with given initial conditions. We determine the solutions by following known techniques from Strauss (2008) and recently acquired procedures from Walsh (2011). We utilize methods presented by Dean & Dalrymple (1991) to analyze our results. Furthermore, we learn and use the computational software system Mathematica to graphically represent the solutions to the mathematical models. Using mathematical programs (Henderson, private communication), we compare our graphical representations to the laboratory measurements.

In the William G. Pritchard Fluid Mechanics Lab in the Mathematics Department, we conduct physical experiments using the 50ftx10in wave channel. The water depth is 5.5 cm. To initiate the propagation of a wavetrain in the wave channel, a system fabricated with a submerged plate of known thickness abruptly lowers or raises a given distance. We obtain measurements of the evolution of the surface displacement as a function of distance from the plate using capacitance-type wave gages. We qualitatively compare the measurements from the experiments to the graphical representations of solutions of the KdV equation using Mathematica.

§III. The Fully- Nonlinear Water Wave Boundary Value Problem

We consider the fully nonlinear BVP for water waves, first posited by Stokes (1847), and solve its linearization to determine the dispersion relation between frequency and wavelength as well as a description of the surface displacement. In this model, we ignore the motions of the air. Further, we assume that the water is an incompressible and inviscid fluid, with irrotational motions. Mathematically, an incompressible velocity field has zero divergence, and irrotational flow signifies zero curl. Since the velocity field of the water particles is incompressible and irrotational, we can introduce the velocity potential $\phi(x, z, t)$ and reduce the number of unknowns by one. Thus, the statement of conservation of mass reduces to Laplace's equation

$$\Delta\phi = \phi_{xx} + \phi_{zz} = 0 \text{ on } -\infty < x < \infty, -h < z < \eta(x,t). \tag{1.1}$$

For this two-dimensional model, the wavetrain propagates infinitely along one horizontal direction, x, with a velocity field that varies in the horizontal and vertical, z, directions. The uniform water depth, h, defines the bottom boundary. The vertical velocity, therefore, must vanish at the bottom boundary, $z = -h$. The equation describing no flow through the bottom boundary is given by:

$$\phi_z = 0 \text{ on } z = -h. \tag{1.2}$$

Our model for a monochromatic wave requires periodic boundary conditions in the horizontal dimension and with respect to time. At the free surface, the boundary conditions dictate that particles on the surface stay on the surface and the pressure jump across the interface is balanced by curvature due to surface tension. Using calculus methods from Stewart (2007), we derive the kinematic free surface boundary condition,

$$\eta_t - \phi_z + \eta_x\phi_x = 0 \text{ on } z = \eta(x,t). \tag{1.3}$$

The second boundary condition at the free surface, called the dynamic boundary condition, dictates a balance of pressure across the surface, which varies due to the restoring forces of gravity and capillarity. This condition is given by:

$$\phi_t + g\eta + \frac{1}{2}[(\phi_x)^2 + (\phi_z)^2] = T\frac{\eta_{xx}}{[1 + (\eta_x)^2]^{3/2}} \text{ on } z = \eta(x,t), \tag{1.4}$$

where g is the acceleration of gravity and T is the coefficient of the kinematic surface tension. The two free surface boundary conditions describing our system are nonlinear. Not only do these two equations contain nonlinear terms, but they are also evaluated at an unknown boundary, $z = \eta(x,t)$. To model the main physics, we linearize the problem in §III.1.

§III.1. The Linearized Problem

The linearized problem is given by (1.1), (1.2), and the following two linearized versions of the boundary conditions evaluated on the quiescent surface:

$$\eta_t - \phi_z = 0 \text{ on } z = 0 \tag{1.5}$$

and

$$\phi_t + g_\eta = T\eta_{xx} \text{ on } z = 0. \tag{1.6}$$

We use separation of variables to solve Laplace's equation (1.1) subject to the bottom boundary condition (1.2) and periodic boundary conditions in x. First, we assume a product of solutions of the form:

$$\phi(x,z,t) = X(x)Z(z)Y(t). \tag{1.7}$$

Then, Laplace's equation (1.1) becomes

$$X''(x)Z(z)Y(t) + X(x)Z''(z)Y(t) = 0. \tag{1.8}$$

Requiring $Y(t) \neq 0$ and using algebraic simplification, we obtain

$$\frac{X''(x)}{X(x)} = \frac{-Z''(z)}{Z(z)} = \lambda, \tag{1.9}$$

where λ is an arbitrary constant. Since we have a function dependent only on x equal to a function dependent only on z, these functions must both be equal to the same constant. By the method of separation of variables, we have reduced the original PDE to equations involving ordinary derivatives. Since λ is a constant, we find the solutions to each corresponding ordinary differential equation (ODE) subject to the boundary conditions for different sign restrictions. To avoid the trivial solution and to find solutions periodic in x, we select the case where λ is nonzero and negative. Thus, we consider each side of the equation separately and obtain the following two ODEs for $\lambda = -k^2 < 0$:

$$X''(x) + k^2X(x) = 0 \tag{1.10}$$

and

$$Z''(z) - k^2Z(z) = 0. \tag{1.11}$$

The corresponding solutions are

$$X(x) = A\cos(kx) + B\sin(kx) \tag{1.12}$$

and

$$Z(z) = C\cosh(kz) + D\sinh(kz), \tag{1.13}$$

where $A, B, C,$ and D are constants. To determine more information about the solution, we apply the boundary conditions. By periodicity, we define $k = \frac{2\pi}{L_x}$, where k represents wavenumber and L_x is the wavelength. We evaluate $\phi_z = 0$ at $z = -h$ and use our results to obtain

$$\phi(x, z, t) = [\hat{A}cos(kx) + \hat{B}sin(kx)]\cosh(kh + kz)Y(t). \tag{1.14}$$

We use a combination of the linearized free surface boundary conditions (1.5-1.6) to determine $Y(t)$. After algebraic manipulation of the linear free-surface boundary conditions, we obtain an equation in terms of the velocity potential, given by:

$$g\phi_z = T\phi_{xxz} - \phi_{tt} \text{ on } z = 0. \tag{1.15}$$

We determine respective derivatives of (1.14) evaluated at $z = 0$ and substitute them into (1.15) to obtain

$$Y''(t) + [gk\tanh(kh) + Tk^3\tanh(kh)]Y(t) = 0. \tag{1.16}$$

The solution to (1.16) is

$$Y(t) = E\cos(\omega t) + F\sin(\omega t), \tag{1.17}$$

where E and F are constants,

$$\omega^2 = gk\tanh(kh) + Tk^3\tanh(kh) \tag{1.18}$$

is the radian frequency, and (1.18) is called the dispersion relation. It is the relationship between wave frequency and wavelength, $L_x = \frac{2\pi}{k}$.

Hence, we can write our solution as

$$\phi = \left[\hat{A}\cos(kx) + \hat{B}\sin(kx)\right]\cosh(kh + kz)[E\cos(\omega t) + F\sin(\omega t)]. \tag{1.19}$$

To solve for the free surface displacement, $\eta(x,t)$, we use (1.5) and (1.19). Taking the partial derivative with respect to z of the velocity potential (1.19) and integrating the differentiated function with respect to t gives

$$\eta(x,t) = \left[\hat{A}\cos(kx) + \hat{B}\sin(kx)\right]k\sinh(kh)\left[\frac{E}{\omega}\sin(\omega t) - \frac{F}{\omega}\cos(\omega t)\right]. \tag{1.20}$$

We can combine some constants, use trigonometric identities, and ignore the waves moving in the left horizontal direction. In our model, we only consider waves that propagate from left to right, which corresponds to the positive x-direction. Thus, we can rewrite our solution as

$$\eta(x,t) = a_0\cos(kx - \omega t + \theta_0), \tag{1.21}$$

where a_0 is the amplitude of the linearized wave and θ_0 is the wave's phase shift. Following similar procedures and applying the kinematic boundary condition, we can rewrite the velocity potential as

$$\phi(x,z,t) = a_0\frac{\omega}{k}\sin(kx - \omega t + \theta_0)\frac{\cosh[k(h+z)]}{\sinh(kh)}. \tag{1.22}$$

§III.2. Limits of the Solution

Here, we consider various limits of the dispersion relation (1.18) to gain insight on the behavior of waves for their respective water depth. We determine the corresponding dispersion relation by computing the deep-water and shallow-water limit for waves.

For deep-water waves, the wavelength is short compared to the depth. Thus, $kh \gg 1$, where $k = \frac{2\pi}{L_x}$ represents the wavenumber and L_x is the wavelength. In this limit, $\lim_{kh\to\infty}\tanh(kh) = 1$, which implies that $\omega^2 = gk + Tk^3$. The phase speed, $c_p = \frac{\omega}{k}$, becomes $c_p = \frac{\sqrt{gk+Tk^3}}{k}$ for deep-water waves. Since the speed of the waves depends on the wavelength, deep-water waves are dispersive.

Shallow-water waves correspond to waves with long wavelengths in comparison to the depth, such that $kh \ll 1$. We use Taylor Series expansion to obtain $\lim_{kh\to 0}\tanh(kh) = kh$.

In the case of shallow water, the dispersion relation is $\omega^2 = gk^2h + Tk^4h$ and the wave speed is $c_p = \sqrt{gh + Tk^2h}$.

If surface tension dominates gravity, then phase speed depends on the wavelength, so the waves are dispersive. However, shallow-water gravity waves, which have gravitation as the dominating restoring force, are non-dispersive. Their speeds for all wavelengths is $c_p = \sqrt{gh}$.

An initial surface deformation initiates a response from the restoring forces, gravitation and surface tension, and causes waves to form on the surface. Ripples refer to waves for which the two restoring forces are near being balanced. The wavelength corresponding to the balance of gravitation and capillary forces can be calculated from the dispersion relation. For ripples in deep water, we rewrite (1.18) as

$$\omega^2 = gk(1 + \frac{Tk^2}{g}) \tag{1.23}$$

We set $\frac{Tk^2}{g} = 1$ and obtain the wavenumber, $k = 3.634$ cm, and wavelength, $L_x = 1.728$ cm.

§III.3. Graphs of Solutions

Consider the dispersion relation for deep-water waves. We previously defined the phase speed for deep-water waves to be $c_p = \frac{\sqrt{gk+Tk^3}}{k}$. Figure 1 shows a graph of the dispersion relation in the form of phase speed as a function of k.

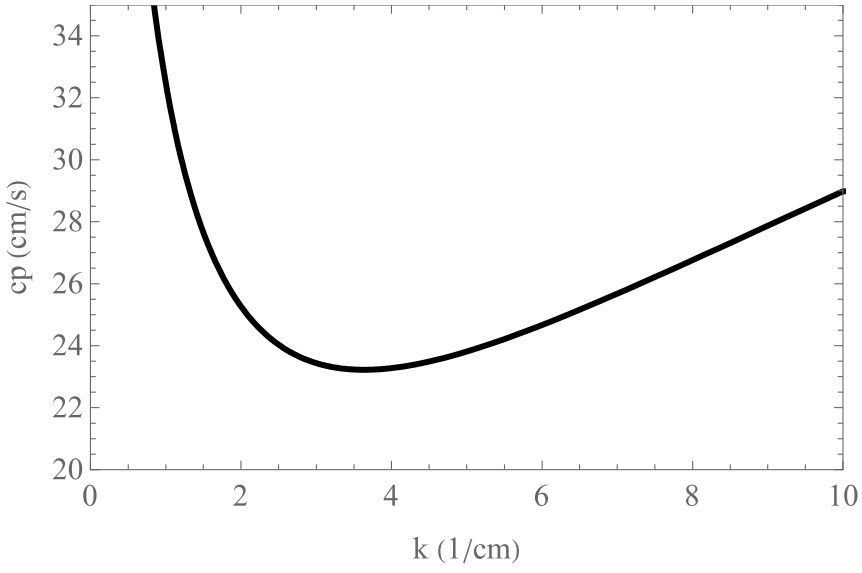

Figure 1—Phase Speed Graph

Using the equation for the dispersion relation of deep-water waves (1.23), we can compute the values of the wavenumber, k, and wavelength, L_x, for various frequencies,

$f = 0.1, 1, 3, 5, 10\ Hz$, where $f = \frac{\omega}{2\pi}$ is the cyclic frequency. We use values for the acceleration of gravity as $g = 980\ \frac{cm}{s^2}$ and for the coefficient of the kinematic surface tension as $T = 74.2\ \frac{cm^3}{s^2}$. Using Newton's Method learned from Stewart (2007), we solve for the wavenumber. Results are listed in Table 1.

f (cycle/s)	$\omega(1/s)$	$k(1/\text{cm})$	$L_x(\text{cm})$
0.1	0.2π	0.004	15597.18
1	2π	0.04	155.99
3	6π	0.359	17.49
5	10π	0.943	6.65
10	20π	2.638	2.38

Table 1— Wavenumber and Wavelength for Varying Frequencies

Consider a monochromatic wavetrain with a frequency of 3 Hz. Figure 2 shows a graph of the free surface, η (1.20), as a function of x at a fixed time $t = 0$, and for $\phi_0 = 0$.

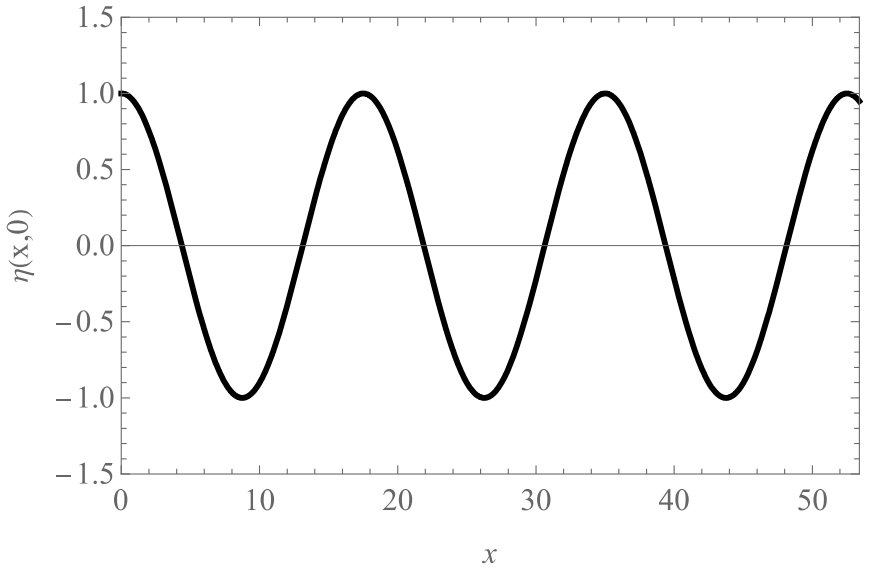

Figure 2—A Monochromatic Wavetrain with Frequency 3 Hz

§IV. The KdV Equation for Shallow-water Waves

In the case of shallow-water waves, one allows for weak dispersion and weak nonlinearity to derive the KdV equation. In §III.2, the shallow-water limit provided an approximation for the dispersion relation that neglects dispersion. To allow for weak dispersion, we evaluate the limit including the first two terms of the Taylor series expansion for $\tanh(kh)$. Thus, $\lim_{kh\to 0} \tanh(kh) = kh + \frac{1}{3!}(kh)^3$. Additionally, we allow for weak nonlinearity by using an asymptotic expansion in a small parameter, ε. Following Walsh (2011), we define the slow

variables, $\psi = \varepsilon\frac{1}{h}(x - c_0 t)$ and $\tau = \varepsilon\frac{c_0}{6h}t$, which correspond to slow changes in space and time, in terms of $\varepsilon \ll 1$. Models of the slow evolution of wave amplitudes is given by the KdV equation:

$$u_\tau + 6uu_\psi + u_{\psi\psi\psi} = 0, \tag{2.1}$$

where $u(\psi, \tau) = \frac{3}{2h}\eta$ corresponds to the wave amplitude.

§IV.1. The Soliton Solution

Following Strauss (2008), we determine a soliton solution of the KdV equation. We anticipate a traveling wave solution $u(\psi, \tau) = f(\zeta)$, where $\zeta = \psi - c\tau$ and c refers to a constant speed. Rewriting (2.1), we obtain an ODE,

$$-cf' + 6ff' + f''' = 0. \tag{2.2}$$

After integrating, (2.2) becomes

$$-cf + 3f^2 + f'' = a, \tag{2.3}$$

where a is a constant of integration. Next, we multiply both sides of (2.3) by $2f'$ and integrate the resulting product to obtain

$$-cf^2 + (f')^2 + 2f^3 = 2af + b, \tag{2.4}$$

where b is a constant.

We look for a solitary wave solution. Because this solution is localized such that the surrounding water has no elevation, the function f and its derivatives tend to 0 as $\psi \to \pm\infty$. Therefore, we must set, $a = b = 0$, which gives

$$-cf^2 + (f')^2 + 2f^3 = 0. \tag{2.5}$$

From (2.5), we can derive the solution

$$u(\psi, \tau) = \frac{c}{2}\operatorname{sech}^2[\frac{1}{2}\sqrt{c}(\psi - c\tau - \psi_0)]. \tag{2.6}$$

In laboratory coordinates, this becomes

$$\eta(x, t) = a_0 \operatorname{sech}^2[\sqrt{\frac{3a_0}{4h^3}}\left(x - c_0 t\left(1 + \frac{a_0}{2h}\right) - x_0\right)], \tag{2.7}$$

where $c_0 = \sqrt{gh}$ and x_0 is an arbitrary constant. From this solution, we observe, as a result of nonlinearity, that solitons with increasing amplitude travel with increasing speed.

§IV.2. The General Solution

We now linearize the KdV equation (2.1) so that we can analyze the behavior of additional, approximate solutions. We obtain

$$u_\tau + u_{\psi\psi\psi} = 0. \tag{2.8}$$

To assess the dispersion relation for the linearized KdV equation, we consider oscillatory waves given by

$$u \sim e^{i(\omega\tau - k\psi)}. \tag{2.9}$$

Substituting (2.9) into (2.8) results in the following equations for the dispersion relation

$$\omega = -k^3, \tag{2.10}$$

and for the phase speed

$$c(k) = -k^2. \tag{2.11}$$

Here, allowing for weak dispersion decreases the speed of the waves. Waves influenced by dispersive effects tend to break up into a train of waves. Weak nonlinearity competes with weak dispersion by causing the waves to steepen and increases the speed of the waves. When both effects are acting on a wave, the wave remains in a stable form. When nonlinearity and dispersion are in perfect balance, one obtains the KdV equation.

Since (2.8) is linear with constant coefficients, we can use Fourier transforms to find solutions. Applying the forward Fourier Transform, we obtain

$$u(\psi, \tau) = \int_{-\infty}^{\infty} A(k, \tau) e^{-ik\psi} dk. \tag{2.12}$$

After substituting (2.12) into (2.8) and simplifying, we find the solution for $A(k, \tau)$, given by

$$A(k, \tau) = A_0 e^{ik^3\tau}, \tag{2.13}$$

where A_0 is a constant, determined by the initial data. If we apply the Fourier transform to the initial conditions, we obtain

$$A_0(k) \equiv A(k, 0) = \int_{-\infty}^{\infty} f_0(\psi) e^{-ik\psi} d\psi. \tag{2.14}$$

and by inverse Fourier transforms,

$$u_0(\psi) \equiv u(\psi, 0) = \frac{1}{2\pi} \int_{-\infty}^{\infty} A(k) e^{ik\psi} dk. \tag{2.15}$$

Thus, the general solution for an initial condition given by u_0 is

$$u(\psi, \tau) = \frac{1}{2\pi} \int_{-\infty}^{\infty} A_0(k) e^{(ik\psi + ik^3\tau)} dk. \tag{2.16}$$

§IV. 3. Solutions for Given Initial Data

In this section, we look for solutions of the linearized KdV equation for two initial conditions. The first condition is an initial upward elevation, and the second condition is an initial downward movement. To find solutions, we substitute these initial conditions into the general equations obtained using Fourier transforms.

First, we look at an initial positive-displacement rectangular wave of the form

$$u_0(\psi) = \alpha[H(\psi + 2\lambda) - H(\psi)], \tag{2.17}$$

where H is the Heaviside step function given by

$$H(\psi - \psi_0) = \begin{cases} 1, & \psi > \psi_0 \\ 0, & \psi < \psi_0. \end{cases} \tag{2.18}$$

To find a solution to the linear KdV equation, we substitute this initial condition into (2.14) to obtain

$$A_0(k) = \int_{-2\lambda}^{0} \alpha\, e^{-ik\psi}\, d\psi. \tag{2.19}$$

After evaluating the integral, we find

$$A_0(k) = \frac{\alpha i}{k} e^{ik\lambda}[e^{-ik\lambda} - e^{ik\lambda}]. \tag{2.20}$$

Rewriting the complex exponential function as a trigonometric function, we obtain

$$A_0(k) = \frac{2\alpha}{k} e^{ik\lambda} \sin(k\lambda), \tag{2.21}$$

which implies that the solution corresponding to (2.17) is

$$u(\psi, \tau) = \frac{\alpha}{\pi} \int_{-\infty}^{\infty} \frac{\sin(k\lambda)}{k} e^{ik\lambda + ik\psi + ik^3\tau}\, dk. \tag{2.22}$$

Second, we consider a negative-displacement rectangular wave of the form

$$u_0(k) = \alpha[H(\psi) - H(\psi + 2\lambda)], \tag{2.23}$$

Which is (2.17) multiplied by -1. Therefore, the solution for this initial condition is the negative solution of the first initial condition, which is given by

$$u(\psi, \tau) = -\frac{\alpha}{\pi} \int_{-\infty}^{\infty} \frac{\sin(k\lambda)}{k} e^{ik\lambda + ik\psi + ik^3\tau}\, dk. \tag{2.24}$$

To understand the nature of the water surface displacement, we examine the behavior of the solution near the wave front for long-time solutions, such that $\tau \to \infty$.

The waves we observe near the wave front, for which $\psi \to 0$, include the waves with the fastest speeds. Recall that the wave speed results from a ratio of frequency to wavenumber. Hence, the fastest waves correspond to small values of k. Correspondingly, we seek waves such that $k \approx 0$. We rewrite our general solution (2.16) by introducing the following similarity variables:

$$\xi = \frac{\psi}{(3\tau)^{1/3}}, \tag{2.25}$$

$$\kappa = k(3\tau)^{1/3}, \tag{2.26}$$

and $g(\xi, \tau) = u(\psi, \tau)$ to obtain

$$g(\xi, \tau) = \frac{(3\tau)^{-1/3}}{2\pi} \int_{-\infty}^{\infty} A_0[\frac{\kappa}{(3\tau)^{1/3}}] e^{ik\xi + \frac{ik^3}{3}}\, dk. \tag{2.27}$$

With further computation, we determine the value of τ that provides information on the asymptotic behavior of the waves. For an approximation about $k \approx 0$, we use Taylor series to obtain

$$A_0(k) \sim A_0(0) + kA'_0(0) + \frac{k^2}{2} A''_0(0) + \cdots \tag{2.28}$$

We can rewrite the general solution in terms of the similarity variables using this approximation for $A_0(k)$. Considering (2.28), we rewrite (2.27) as

$$\begin{aligned} g(\xi, \tau) = \frac{1}{(3\tau)^{1/3}} \Bigg\{ & A_0(0) \frac{1}{2\pi} \int_{-\infty}^{\infty} e^{i\left(\kappa\xi + \frac{1}{3}\kappa^3\right)}\, d\kappa \\ & + \frac{A'_0(0)}{(3\tau)^{1/3}} \frac{1}{2\pi} \int_{-\infty}^{\infty} \kappa e^{i\left(\kappa\xi + \frac{1}{3}\kappa^3\right)}\, d\kappa \\ & + \frac{A''_0(0)}{2(3\tau)^{2/3}} \frac{1}{2\pi} \int_{-\infty}^{\infty} \kappa^2\, e^{i\left(\kappa\xi + \frac{1}{3}\kappa^3\right)}\, d\kappa + \cdots \Bigg\}, \end{aligned} \tag{2.29}$$

which we can further rewrite in terms of the Airy function:

$$Ai(\xi) := \frac{1}{2\pi} \int_{-\infty}^{\infty} e^{i(\kappa\xi + \frac{1}{3}\kappa^3)}\, d\kappa, \tag{2.30}$$

such that (2.29) becomes

$$g(\xi, \tau) = \frac{A_0(0)}{(3\tau)^{1/3}} Ai(\xi) + \frac{A'_0(0)}{i(3\tau)^{2/3}} Ai'(\xi) - \frac{A''_0(0)}{2(3\tau)} Ai''(\xi) + O\left(\frac{1}{(3\tau)^{4/3}}\right). \tag{2.31}$$

We can simplify (2.31) for the respective initial data. The solution for the positive initial condition, graphed in Figure 3, is

$$g(\xi,\tau)=\frac{2\alpha\lambda}{(3\tau)^{1/3}}\left[Ai(\xi)+\frac{\lambda}{(3\tau)^{1/3}}Ai'(\xi)-\frac{\frac{2}{3}\lambda^2}{(3\tau)^{2/3}}Ai''(\xi)+\cdots\right]. \tag{2.32}$$

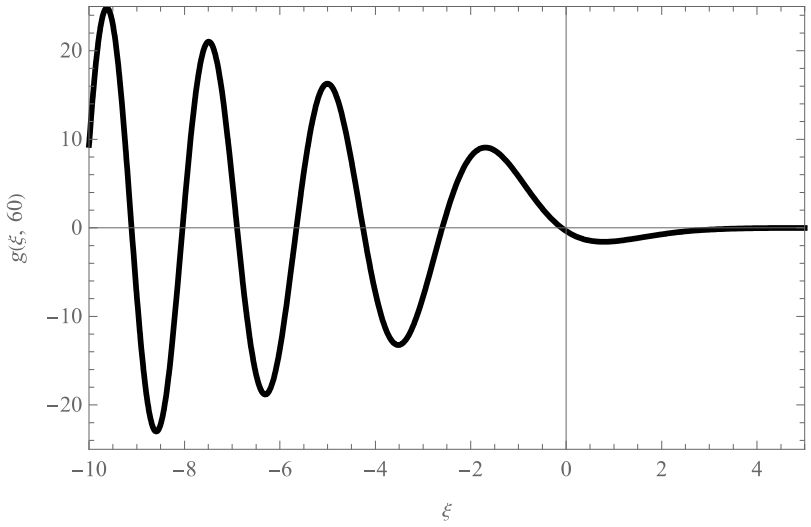

Figure 3—Solution for Initial Positive Displacement

The solution for the negative initial condition, graphed in Figure 4, is

$$g(\xi,\tau)=\frac{-2\alpha\lambda}{(3\tau)^{1/3}}\left[Ai(\xi)+\frac{\lambda}{(3\tau)^{1/3}}Ai'(\xi)-\frac{\frac{2}{3}\lambda^2}{(3\tau)^{2/3}}Ai''(\xi)+\cdots\right]. \tag{2.33}$$

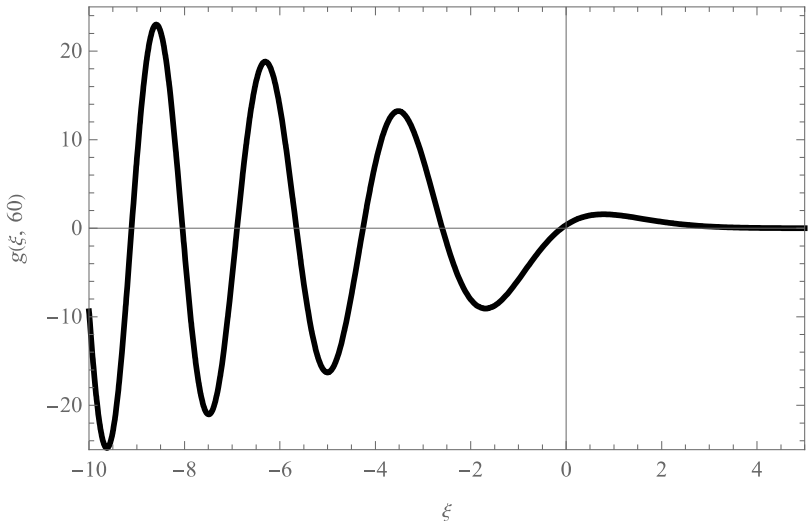

Figure 4—Solution for Initial Negative Displacement

§IV. 4. Experiments

We conducted nine experiments for which the water in the channel was $h = 5.5$ cm. We used a plastic hand-held box to generate solitons and waves corresponding to the initial data. Table 2 shows the amplitudes of the first three peaks observed in the experiments.

Experiment	Information	Amp 1 (cm)	Amp 2 (cm)	Amp 3 (cm)
E1	2.45 cm	0.397	0.183	0.151
E2	8.45 cm	2.296	1.070	0.940
E3	6.50 cm	1.472	0.776	0.631
E4	4.00 cm	0.837	0.480	0.416
E5	Lowered	0.609	0.310	0.317
E6	Lowered	0.739	0.569	0.429
E7	Lowered	0.683	0.342	0.283
E8	Raised	-0.191	-0.150	-0.092
E9	Raised	-0.733	-0.392	-0.275

Table 2— Experimental Data. For E1-E4, the second column lists the horizontal distance traveled by the box. For E5-E9, the second column indicates whether the box was raised or lowered.

To generate a soliton, we pushed the submerged box, which was placed at one end of the tank, forward. In E1, the box was moved 2.45 cm in the direction of the gages. We compare the experimental data, denoted by the black line, to the anticipated solution, identified by the colored line. Figure 5 shows this comparison for the first soliton peak in the second gage data.

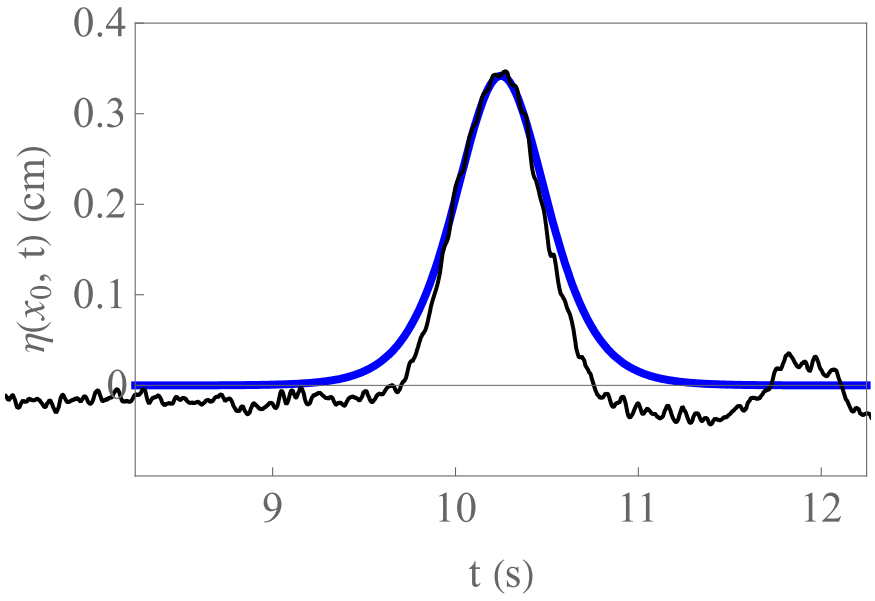

Figure 5—Comparison of E1 and the Soliton Solution (2.7)

E2 follows the same procedure as E1, but the distance of the box changes. The displacement of the box was 8.45 cm for the second experiment. Figure 6 compares the data collected on the second soliton wave and the corresponding solution.

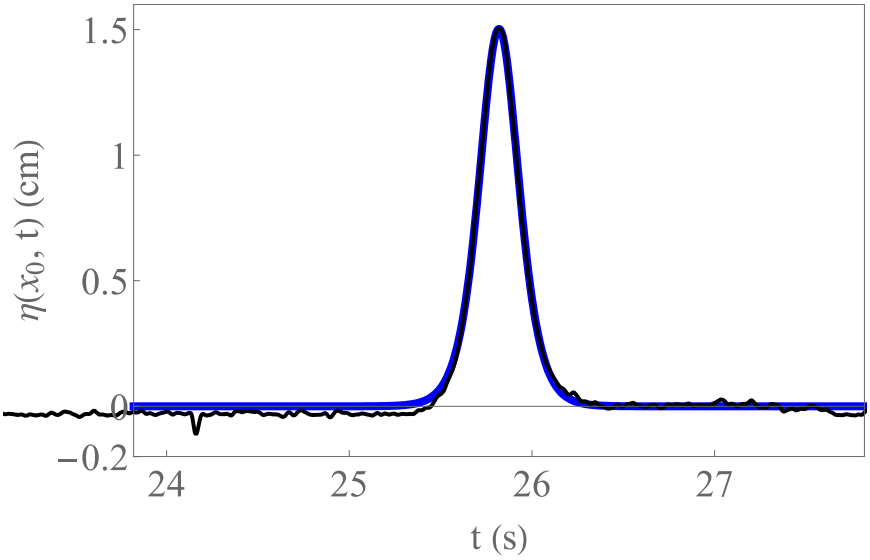

Figure 6—Comparison of E2 and the Soliton Solution (2.7)

For E3, we repeated the same steps, but we pushed the box 6.5 cm. Figure 7 shows a comparison of the data and soliton solution.

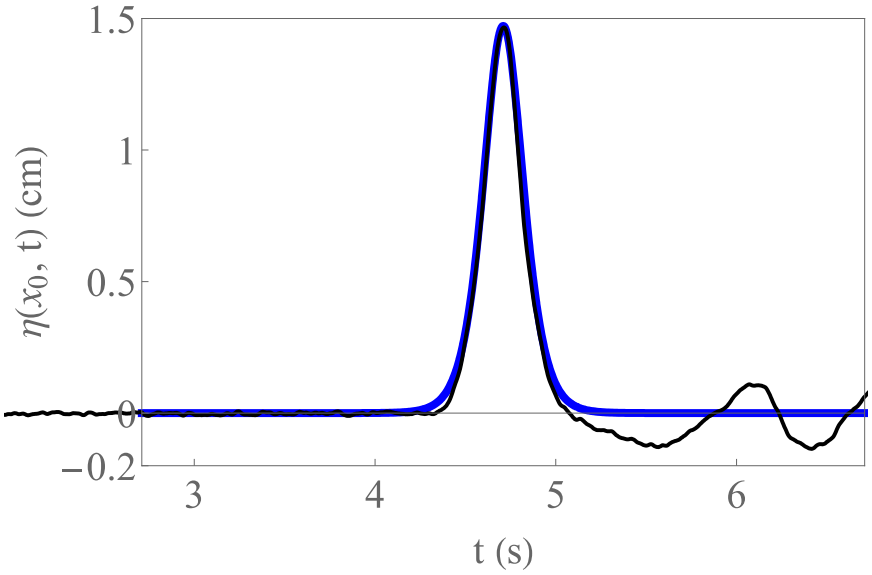

Figure 7—Comparison of E3 and the Soliton Solution (2.7)

In E4 we pushed the box 4.0 cm forward to generate a soliton wave. We compare the collected measurements again with our solution, shown in Figure 8.

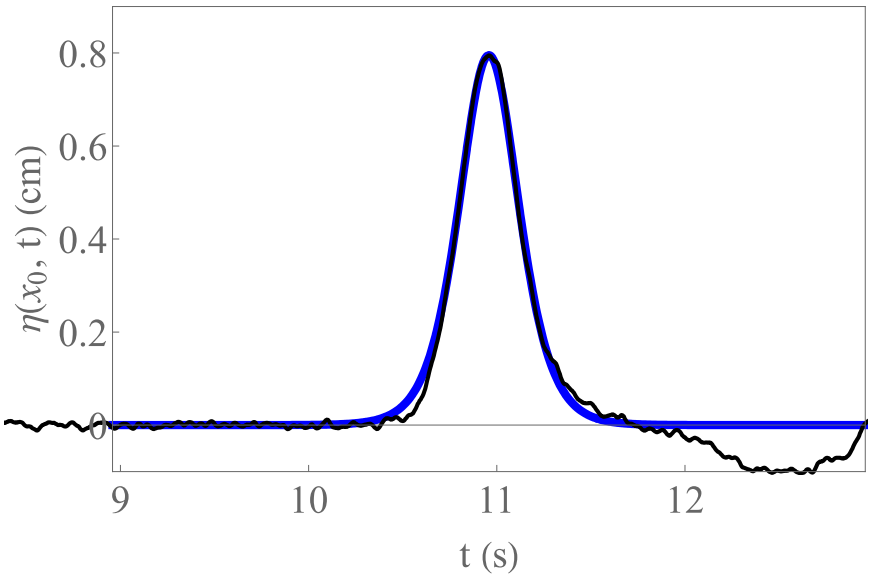

Figure 8—Comparison of E4 and the Soliton Solution (2.7)

For the soliton experiments, we notice agreement between the experimental measurements and the analytic solutions of the full KdV equation. Agreement is qualitatively better for the larger amplitude solitons. A next step would be to do an error analysis to make a quantitative comparison. Further horizontal distances traveled by the box increase the quality of the comparison. The graphed soliton in Figure 6 shows the most agreement, and it corresponds to the E2 data. As shown in Table 2, the soliton with the largest amplitude was generated in E2, which is the experiment where the box traveled the furthest horizontal distance. Figure 9 shows a zoomed in view of the comparison originally shown in Figure 6.

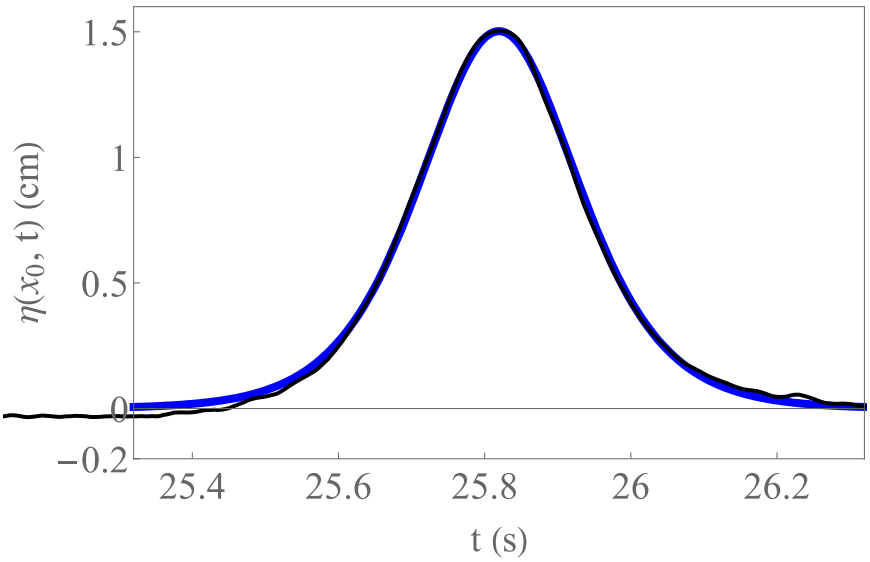

Figure 9—Closer Look at the E2 Data

In E5-E9, we consider a train of waves developed under different initial conditions. For E5, we held the box entirely above the surface of the water and abruptly pushed the long edge (25.4 cm) of the box down to the bottom of the tank and let go, allowing it to float back up. Figure 10 shows the soliton shape of the wave generated in this experiment.

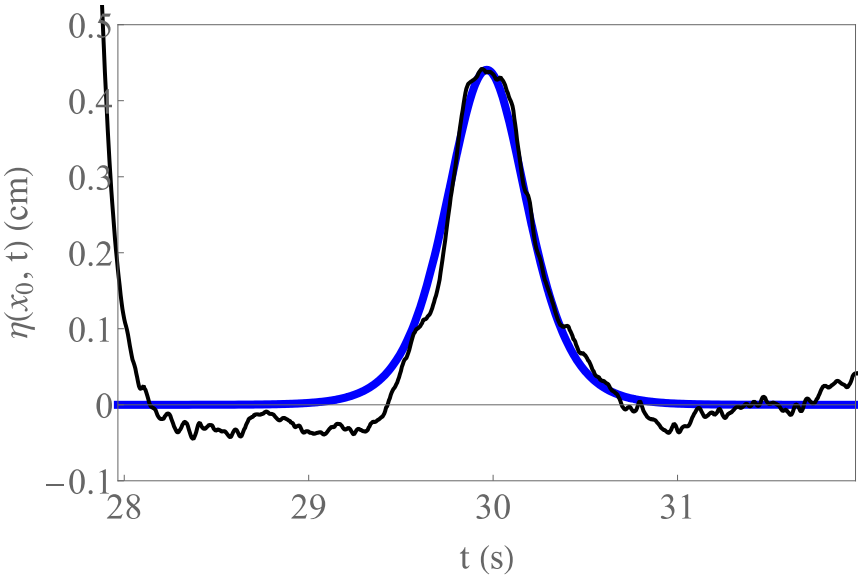

Figure 10—Comparison of Experiment 5 and the Soliton Solution (2.7)

In E6, we repeated the previous experiments method for creating waves by the lowering of a box but held the box fixed on the bottom. Here, we observe two individual solitons evolving along with a train of waves. Figure 11 shows the measured time series. The initial movement is upwards because of an initial negative displacement from dropping the box into the water. E7 considers waves generated by plate depression involving the short edge (10 cm) of the plastic box. The waves in this experiment initiate with a soliton followed by a dispersive wavetrain. Figure 12 portrays the data collected from this experiment.

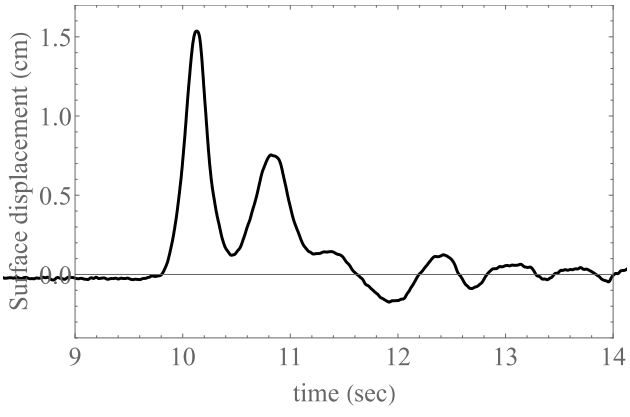

Figure 11—E6

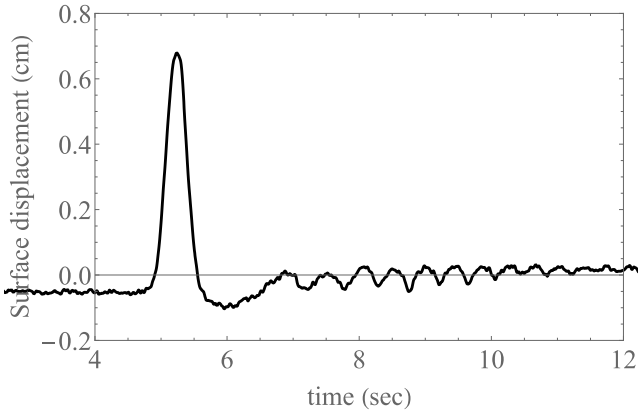

Figure 12—E7

For E8 and E9, we abruptly lifted the box out of the water to generate waves in the tank. We placed the box vertically in the water and lifted it straight out of the tank. We notice an initial downward movement of the water caused by lifting the box. This is the opposite effect observed in the initial downward movement conditions. Figure 13 provides a look at the data collected from E8, where the box was lifted away from the corner of the tank, so that reflections occurred. Figure 14 shows the experimental observations of E9, for which the box lift occurred in the corner of the tank, so that reflections did not occur. The initial positive wave for a negative initial condition and negative wave for a positive initial condition is consistent with predictions from our solutions from (2.27).

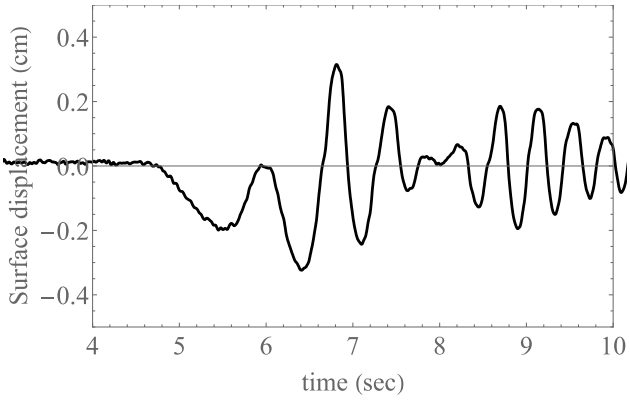

Figure 13—E8

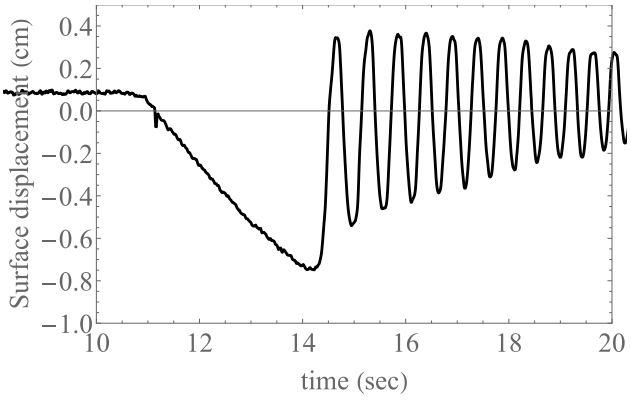

Figure 14—E9

Discussion

Through our investigation, we developed an understanding of the dispersion of waves in various depths and the evolution of shallow-water waves. Solutions to the linearized version of the boundary value problem for water waves provide insight into the behavior of a train of waves at a water surface. Various limits of the solution reveal the relationship between wave speed and wavelength, which explains the non-dispersive property of shallow-water gravity waves. Evaluation of the KdV equation for shallow-water waves provides a theoretical insight into the stable form and speed of a soliton. The data from the experiments that generate a soliton agree reasonably well with the soliton solution of the KdV equation. For the experiments that consider wave propagation caused by abruptly pushing a plastic box down into the water, the measurements of surface displacement agree qualitatively with our predicted solution for initial conditions as do waves obtained from the abrupt raising of the box out of the water.

References

Dean, R. G., & Dalrymple, R. A. (1991). *Water Wave Mechanics for Engineers and Scientists*. World Scientific Publishing Company.

Hammack, J. L. & Segur, H. (1978). The Korteweg-de Vries equation and water waves. Part 3. Oscillatory waves. *Journal of Fluid Mechanics*, 84(2), 337-358. doi:10.1017/S0022112078000208.

Henderson, D. M. (2022). Private Communication.

Stewart, J. (2007). *Essential calculus: Early transcendentals.* Belmont, CA: Thomson Higher Education.

Stokes, G. G. (1847). On the Theory of Oscillatory Waves. *Transactions of the Cambridge Philosophical Society*, 8, and Supplement. Scientific Papers, 1.

Strauss, W. 2008. *Partial Differential Equations: An Introduction*, *2nd Edition*. New York: Wiley and Sons.

Walsh, M. E. (2011). *The propagation of shallow-water waves*. (Undergraduate Thesis, the Pennsylvania State University).